# Kinetic Analysis of YPD1-Dependent Phosphotransfer Reactions in the Yeast Osmoregulatory Phosphorelay System†

Fabiola Janiak-Spens, Paul F. Cook, and Ann H. West*

*Department of Chemistry and Biochemistry, University of Oklahoma, Norman, Oklahoma 73019*

*Received July 22, 2004; Revised Manuscript Received October 1, 2004*

ABSTRACT: In *Saccharomyces cerevisiae*, the histidine-containing phosphotransfer (HPt) protein YPD1 transfers phosphoryl groups between the three different response regulator domains of SLN1, SSK1, and SKN7 (designated R1, R2, and R3, respectively). Together these proteins form a branched histidine−aspartic acid phosphorelay system through which cells can respond to hyperosmotic and other environmental stresses. The in vivo order of phosphotransfer reactions is believed to proceed from SLN1-R1 to YPD1 and then subsequently to SSK1-R2 or SKN7-R3. The individual phosphoryl transfer reactions between YPD1 and the response regulator domains have been examined kinetically. A maximum forward rate constant of 29 $s^{-1}$ was determined for the reaction between SLN1-R1∼P and YPD1 with a $K_d$ of 1.4 $\mu$M for the SLN1-R1∼P·YPD1 complex. In the subsequent reactions, phosphotransfer from YPD1 to SSK1-R2 is very rapid (160 $s^{-1}$) and is strongly favored over phosphotransfer to SKN7-R3. Phosphotransfer reactions between YPD1 and SLN1-R1 or SKN7-R3 were reversible. In contrast, no reverse transfer from SSK1-R2∼P to YPD1 was observed. These findings are consistent with the notion that SSK1 is constitutively phosphorylated under normal osmotic conditions. In addition, we have examined the roles of several conserved amino acid residues surrounding the phosphorylatable histidine (H64) of YPD1 using phosphoryl transfer reactions involving YPD1 mutants. With respect to phosphoryl transfer from SLN1-R1∼P, only one YPD1 mutant (K67A) exhibited an increase in $K_d$ and thus affects binding of YPD1 to SLN1-R1∼P, whereas other mutants (R90A, Q86A, and G68Q) showed a decrease in phosphoryl transfer rate. Only the G68Q-YPD1 mutant was significantly affected in phosphotransfer to SSK1-R2 (∼680-fold decrease in rate in comparison to wild-type). This is the first report of a kinetic analysis of a eukaryotic "two-component" histidine−aspartic acid phosphotransfer system, enabling a comparison of the transfer rates and binding constants to the few bacterial systems that have been studied this way.

Histidine-containing phosphotransfer (HPt)[1] proteins mediate phosphoryl group transfer from one response regulator protein to another in multistep histidine−aspartic acid phosphorelay systems (*1*, *2*). In the *Saccharomyces cerevisiae* osmoregulation pathway, the HPt protein YPD1 accepts phosphoryl groups from the response regulator domain of the membrane-bound sensor histidine kinase SLN1. Subsequently, phosphoryl groups are transferred from YPD1 to two downstream response regulator proteins, SSK1 and SKN7. Under normal environmental conditions, SSK1 is maintained in an inactive phosphorylated state (*3*). However, when cells experience hyperosmotic stress, SSK1 becomes dephosphorylated and activates the downstream HOG1 mitogen-activated protein (MAP) kinase cascade, which ultimately leads to an increase in the intracellular glycerol concentration (*3*−*7*). The other response regulator, SKN7, functions as a transcription factor and is involved in multiple stress-related responses, not all of which depend on phosphotransfer from YPD1 (*8*−*14*). The hybrid histidine kinase SLN1 contains a histidine kinase domain as well as a C-terminal response regulator domain, designated SLN1-R1. YPD1 shuttles phosphoryl groups from SLN1-R1 to the response regulator domains associated with SSK1 and SKN7, designated SSK1-R2 and SKN7-R3, respectively (*15*, *16*). Information regarding regulatory control and kinetic rates for these reactions, however, is lacking.

Histidine kinases and HPt proteins are the primary phosphoryl group donors for response regulator domains in "two-component" signaling systems (*17*, *18*). Though small molecule phosphodonors, like acetyl phosphate and phosphoramidate, can also serve as substrates for response regulators in vitro (*19*), phosphoryl groups presented on the surface of a protein, that is, a histidinyl phosphate, appear to be the preferred and more efficient substrates (*20*, *21*). To date, all HPt proteins have a four-helix bundle core architecture, which contains the phosphorylatable histidine residue and provides the response regulator binding site. Histidine kinases are identified by an additional ATP-binding/catalytic domain as well as other functional domains.

† This work was supported by a U.S. Public Health Service grant (No. GM59311) to A.H.W. from the National Institutes of Health and a grant from the National Science Foundation to P.F.C. (MCB 009127). A.H.W. is a Cottrell Scholar of Research Corporation.

* Corresponding author. Mailing address: Department of Chemistry and Biochemistry, University of Oklahoma, 620 Parrington Oval, Norman, OK 73019. Telephone: (405) 325-1529. Fax: (405) 325-6111. E-mail: awest@chemdept.chem.ou.edu.

[1] Abbreviations: ATP, adenosine-5′-triphosphate; DTT, dithiothreitol; EDTA, ethylenediaminetetraacetic acid; GST, glutathione-S-transferase; HK, histidine kinase; HPt, histidine-containing phosphotransfer; IPTG, isopropyl β-D-thiogalactopyranoside; PAGE, polyacrylamide gel electrophoresis; PCR, polymerase chain reaction; PMSF, phenylmethanesulfonyl fluoride; SDS, sodium dodecyl sulfate.

10.1021/bi048433s CCC: $30.25 
Published on Web 12/09/2004

HPt proteins from prokaryotes and eukaryotes share little overall sequence homology. However, several amino acid residues in the area surrounding the phosphorylatable histidine are highly conserved among the HPt proteins identified to date (*22*). Furthermore, there is remarkable structural conservation among HPt proteins from prokaryotes and eukaryotes for which structures are known (*22*−*24*). In a previous study, we used structure-based site-directed mutagenesis and in vitro phosphoryl transfer experiments to examine the activities of selected YPD1 mutants in phosphoryl transfer assays (*25*). Functional roles for several of the conserved amino acid residues that surround the phosphorylatable histidine residue, H64, were proposed, but detailed kinetic studies were not performed at that time since most phosphoryl transfer reactions involving YPD1 reached steady-state levels in under 5 s. Using a rapid-quench kinetics instrument, we report here kinetic characterization of the phosphoryl transfer reactions involving YPD1 and each of the three response regulator domains. In addition, YPD1 mutant proteins that exhibited decreased steady-state phosphorylation levels were analyzed to assess the effect of the mutation on phosphotransfer rates, protein binding affinities, or both.

Relatively few two-component regulatory systems, and to our knowledge only one multistep phosphorelay system, have been characterized with respect to kinetic analysis of the individual phosphotransfer steps (*26*−*28*). Thus, comparison of these systems with each other and with the yeast osmoregulatory system presented here will help define similarities and differences of histidine−aspartic acid phosphotransfer reactions that form the basis of two-component signal transduction systems in prokaryotes and eukaryotes.

## EXPERIMENTAL PROCEDURES

*Materials and Methods.* All chemicals and biochemicals used were of ultrapure grade. Glutathione−Sepharose 4B resin and [$\gamma$-$^{32}$P]ATP (30 Ci/mmol) were purchased from Amersham. The SLN1-R1, wild-type and mutant YPD1, SSK1-R2, SKN7-R3, and GST−SLN1-HK proteins were purified as described in the literature (*12*, *15*, *16*, *25*, *29*).

*GST−SLN1-HK-R1 Construction, Expression and Purification.* For protein expression in bacterial cells, the gene fragment corresponding to the cytoplasmic domain of SLN1, containing the histidine kinase (HK) and the C-terminal response regulator (R1) domain, was amplified by PCR and subcloned into the pGEX-KG vector (*30*). Specifically, a plasmid was constructed by cloning a *Sma*I−*Eco*RI fragment containing nucleotides 1587−3660 of the coding region of SLN1 (corresponding to amino acids 530−1220) into pGEX-KG. Thus, an in-frame fusion protein was generated consisting of the SLN1-HK-R1 domains located C-terminal to the glutathione-S-transferase protein. This pGEX-KG derivative was designated pFJS43. Cultures of *Escherichia coli* BL21(DE3)Star cells containing pFJS43 were grown to an $OD_{600}$ of 0.6 at 37 °C; the cultures were then cooled to 16 °C and induced with addition of IPTG to a final concentration of 1 mM. After induction, the cells were grown for an additional 20 h at 16 °C. Cells were harvested, washed, and resuspended in 5 mL per gram of wet cell weight of lysis buffer (50 mM Tris-HCl, pH 8.0, 150 mM NaCl, 1 mM EDTA, 1% Triton X-100, 1 mM PMSF, 1 mM 2-mercaptoethanol, 0.1 $\mu$g/mL chymostatin, 2 $\mu$g/mL aprotinin, 1 $\mu$g/mL pepstatin, 1.1 $\mu$g/mL phosphoramidon, 7.2 $\mu$g/mL E-64 protease inhibitor, 0.5 $\mu$g/mL leupeptin, 2.5 $\mu$g/mL antipain, 100 $\mu$M benzamidine, 100 $\mu$M sodium metabisulfite). Cells were lysed by sonication, and the lysate was clarified by centrifugation at 100 000 × *g* for 1 h at 4 °C. The supernatant was loaded onto a 1 mL glutathione−Sepharose 4B column equilibrated in lysis buffer. The resin was washed with 10 column volumes of lysis buffer followed by 5 column volumes of wash buffer (50 mM Tris-HCl, pH 8.0, 2 mM DTT, 1 mM EDTA) and 5 column volumes of storage buffer (50 mM Tris-HCl, pH 8.0, 100 mM KCl, 1 mM EDTA, 2 mM DTT, 10% glycerol). The resin was then mixed with an equal volume of storage buffer, and the slurry was stored in small aliquots at −20 °C.

*Preparation of Phosphorylated SLN1-R1, SSK1-R2, and SKN7-R3 Proteins.* Phosphorylation of SLN1-R1 was achieved by incubation with the SLN1-HK domain and [$\gamma$-$^{32}$P]ATP. Specifically, GST-tagged SLN1-HK (7 $\mu$M) bound to glutathione−Sepharose 4B resin was incubated with 7 $\mu$M [$\gamma$-$^{32}$P]ATP, 60 $\mu$M unlabeled ATP, and 30 $\mu$M SLN1-R1 in 50 mM Tris-HCl, pH 8.0, 100 mM KCl, 15 mM $MgCl_2$, 2 mM DTT, and 20% glycerol for 30 min at room temperature in a total volume of 100 $\mu$L. Phospho-SLN1-R1 was recovered in the supernatant after a brief centrifugation step (1 min at 100 × *g*) to pellet the GST−SLN1-HK-bound glutathione−Sepharose resin. EDTA was added to the supernatant to a final concentration of 30 mM to prevent autodephosphorylation. Phosphorylation of SSK1-R2 and SKN7-R3 was performed analogously, except that the phosphorylation reaction was incubated for 90 min. All phosphorylated response regulator preparations contained a significant amount of unphosphorylated protein; however, with the exception of the G68Q-YPD1 reaction, no effects of the unphosphorylated protein on the phosphotransfer experiments were observed.

*Preparation of Phospho-YPD1.* Phosphorylation of YPD1 was achieved by incubation with the SLN1-HK-R1 domains and [$\gamma$-$^{32}$P]ATP. Specifically, GST-tagged SLN1-HK-R1 (1 $\mu$M) bound to glutathione−Sepharose 4B resin was incubated with 7 $\mu$M [$\gamma$-$^{32}$P]ATP, 100 $\mu$M unlabeled ATP, and 40 $\mu$M YPD1 in 50 mM Tris-HCl, pH 8.0, 100 mM KCl, 15 mM $MgCl_2$, 2 mM DTT, and 20% glycerol for 90 min at room temperature in a total volume of 100 $\mu$L. Phospho-YPD1 was recovered in the supernatant after a brief centrifugation step (1 min at 100 × *g*) to pellet the GST−SLN1-HK-R1-bound glutathione−Sepharose resin.

*Rapid-Quench Experiments To Monitor Phosphoryl Transfer Reactions.* All rapid-quench experiments were carried out in 50 mM Tris-HCl, pH 8.0, 10 mM $MgCl_2$, and 1 mM DTT at room temperature using a SFM-Q/4 Quench-Flow instrument (BioLogic). For most experiments, phosphorylated protein was diluted to 0.5 $\mu$M in 50 mM Tris-HCl, pH 8.0, 1 mM EDTA, and 1 mM DTT, and 60 $\mu$L of the phosphoprotein sample was mixed with 60 $\mu$L of unphosphorylated protein (0.25−40 $\mu$M) in 50 mM Tris-HCl, pH 8.0, 20 mM $MgCl_2$, and 1 mM DTT. After the reaction was allowed to age for the specified time, 60 $\mu$L of stop buffer (8% SDS, 80 mM EDTA) was added. Similar rapid-quench studies have shown that these quenching reactions were sufficiently faster than the phosphotransfer reactions and thus could be used to determine the phosphotransfer kinetics (*27*). To analyze

Scheme 1

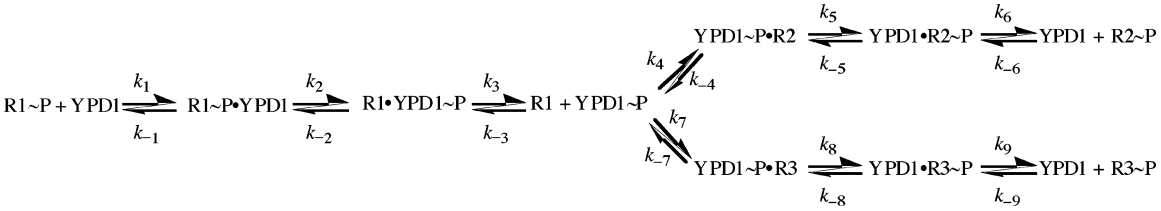


the sample, 30 $\mu$L of the quenched reaction was mixed with 10 $\mu$L of 4× SDS−PAGE sample buffer, and then a 20 $\mu$L sample was loaded onto 15% SDS−PAGE gels. Following gel electrophoresis, wet gels were wrapped in plastic wrap and exposed to phosphorimager screens. The radioactivity in each band was analyzed using a phosphorimager (Molecular Dynamics). Manually mixed phosphoryl transfer experiments were carried out analogously.

Phosphoryl transfer reactions were performed using a series of unphosphorylated (acceptor) protein concentrations while maintaining the phosphorylated (donor) protein concentration constant at 0.25 $\mu$M. The reaction times were controlled by varying the flow of the reactants and stop solution through the delay line as well as by varying the length of the delay line. Each reaction was performed at least twice. The reaction was monitored by the disappearance of $^{32}$P-label from the phosphodonor protein and the appearance of $^{32}$P-label in the phosphoacceptor protein. The kinetic constants were determined by following the disappearance of $^{32}$P-label from the phosphodonor protein. The percent of remaining phosphoprotein was plotted as the natural logarithm versus reaction time. The observed first-order rate constants were obtained by fitting each time course to the linear relationship $\ln A_t = \ln A_0 - kt$, where $A$ is the amount of phosphorylated protein at times $t$ and 0, and $k$ is the rate constant, using the least-squares fitting of Excel (Microsoft Office v. 10.1.2). Estimates of kinetic parameters were obtained using Enzfitter (version 2.04, Biosoft, Cambridge, U.K.) and fitting the individual datasets using eq 1.

$$k_{obs} = k_{rev} + k_{fwd}\left(\frac{[S]}{K_d + [S]}\right) \quad (1)$$

with regard to Scheme 1 (see Results), where [S] is the concentration of phosphate-accepting protein, $k_{obs}$ is the observed first-order rate constant for the transfer reaction at a particular S concentration, $k_{fwd}$ ($k_2$, $k_{-5}$, or $k_{-8}$) is the maximal net forward rate constant for phosphoryl transfer from the phosphorylated response regulator to YPD1, $k_{rev}$ ($k_{-2}$, $k_5$, or $k_8$) is the rate constant for the reaction from phospho-YPD1 to the response regulator, and $K_d$ is the dissociation constant of the phosphoprotein·YPD1 complex. In the cases involving phosphoryl transfer from YPD1 to SSK1-R2 and SKN7-R3 and the phosphotransfer reactions from SLN1-R1 to the mutant YPD1 proteins, where $k_{rev}$ is very slow, the data were fitted to a modified version of eq 1 where $k_{rev}$ is zero.

## RESULTS

*Phosphoryl Transfer from Phospho-SLN1-R1 to YPD1 and Its Reverse Reaction*. The first intermolecular phosphoryl transfer reaction in the yeast osmoregulation pathway occurs between the response regulator domain of SLN1 (SLN1-R1) and the HPt protein YPD1 (Scheme 1).

This reaction consists of, at a minimum, a reversible formation of the encounter complex between phospho-SLN1-R1 and YPD1 ($k_1$ and $k_{-1}$), a reversible chemical transfer step ($k_2$ and $k_{-2}$), and the release of the products SLN1-R1 and phospho-YPD1 ($k_3$). Once phospho-YPD1 is formed ($k_3$), the phosphoryl group can be transferred either in the reverse direction back to SLN1-R1 ($k_{-3}$) or in the forward direction by addition of SSK1-R2 ($k_4$) or SKN7-R3 ($k_7$).

In previous studies, the disappearance of phospho-SLN1-R1 and the appearance of phospho-YPD1 were monitored as a function of time and the phosphoryl transfer reaction was observed to reach steady-state levels in less than 5 s at room temperature, that is, the reaction was too fast to obtain initial velocity data using manual mixing (*25*). Thus, in the present study, a rapid-quench kinetics instrument that facilitates monitoring the reaction at time points in the millisecond range has been employed. For the reaction between phospho-SLN1-R1 (0.25 $\mu$M) and YPD1 (concentrations ranging from 0.125 to 10 $\mu$M), the phosphoryl transfer reaction reaches equilibrium in less than 100 ms, well within the time limits of the rapid-quench instrument. Values for the pseudo-first-order rate constants for the reaction between phospho-SLN1-R1 with YPD1 have been determined by simultaneously monitoring the appearance of phospho-YPD1 and the disappearance of phospho-SLN1-R1 (Figure 1A). The time courses are first-order at all concentrations of YPD1 indicating a rapid formation of the phospho-SLN1-R1·YPD1 complex. Analysis of the data using eq 1 showed saturation kinetics with regard to the YPD1 concentration (Figure 1B), giving a maximum forward rate constant $k_2$ of 29 ± 3 s$^{-1}$ (Table 1). The $K_d$ for the interaction of phospho-SLN1-R1 with YPD1 was 1.4 ± 0.6 $\mu$M. The limiting second-order rate constant, as calculated from the ratio of $k_2/K_d$, was (2.1 ± 0.9) × 10$^7$ M$^{-1}$ s$^{-1}$. For this particular experimental condition, the rate of reverse phosphoryl transfer from YPD1∼P to SLN1-R1 is shown by the $y$-intercept in Figure 1B, and $k_{-2,obs}$ is 7.5 ± 2.9 s$^{-1}$. Since a finite value of $k_{-2}$ was observed, there must be some contribution from $k_3$ to rate limitation, and this will be considered below.

SLN1-R1 can be phosphorylated to a limited extent using small molecule phosphodonors such as acetyl phosphate (F. Janiak-Spens and A. West, unpublished observation), consistent with the commonly accepted notion that phosphoryl transfer catalytic activity resides with the response regulator domain (*19*, *20*, *31*−*33*). The reverse reaction from phospho-YPD1 to SLN1-R1 was performed by varying the concentration of SLN1-R1. At concentrations of SLN1-R1 sufficient to saturate the amount of phospho-YPD1 present, the reaction conditions were those of a single-turnover experiment. A fit of the data to a rectangular hyperbola gave a rate constant

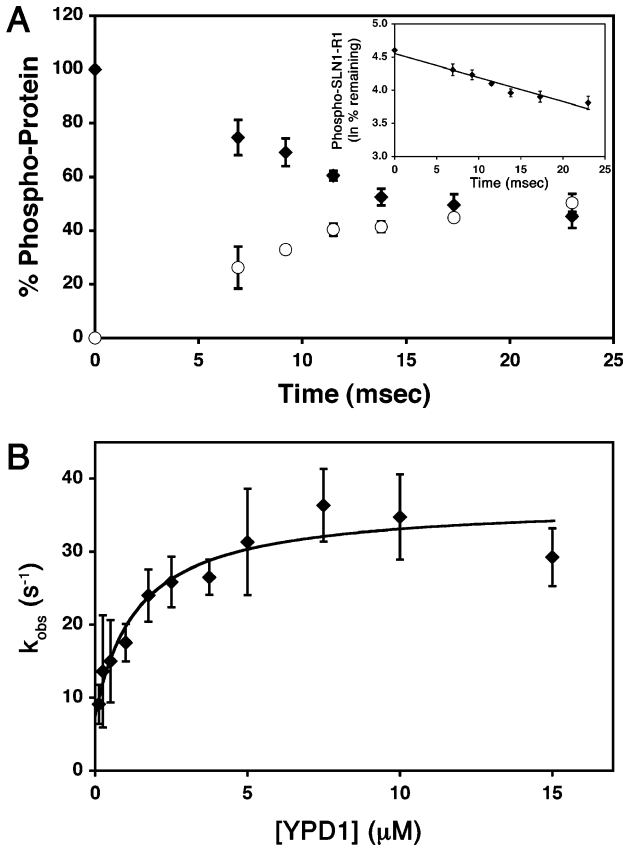


FIGURE 1: Panel A presents a time course of phosphoryl transfer from phospho-SLN1-R1 to YPD1. Radiolabeled phospho-SLN1-R1 (0.5 $\mu$M) was mixed with an equal volume of 15 $\mu$M YPD1 in the rapid-quench instrument, and the reaction was allowed to proceed for the indicated times before addition of quench (stop) solution. The percent of the $^{32}$P-radiolabeled species at each of the time points specified is shown: (○) phospho-YPD1; (◆) phospho-SLN1-R1. The graph shows the average of three experiments. The error bars show the standard error of the mean. The inset shows the percent of phospho-SLN1-R1 remaining, plotted as the natural logarithm versus reaction time. The line shows the result of the computer-generated least-squares fit to a linear relationship to give $k_{obs}$ as the slope of the line. Panel B shows the dependence of the rate of phosphoryl transfer on the concentration of YPD1. The observed pseudo-first-order rate constant ($k_{obs}$), obtained as in panel A, is plotted as a function of YPD1 concentration and shows saturation at high YPD1 concentrations and a finite nonzero ordinate intercept. The curve was created by fitting the data to eq 1. The error bars show the standard error of the mean.

Table 1: Phosphoryl Transfer Rates and Binding Constants for Transfer between Response Regulators and Wild-type YPD1[a]

| transfer reaction | $k_{max}$ ($s^{-1}$)[b] | $K_d$ ($\mu$M) |
|---|---|---|
| P∼SLN1-R1 to YPD1 | 29 ± 3 ($k_2$) | 1.4 ± 0.6 |
| P∼YPD1 to SLN1-R1 | 230 ± 130 ($k_{-2}$) | 7.8 ± 5.7 |
| P∼SSK1-R2 to YPD1 | *c* | *c* |
| P∼YPD1 to SSK1-R2 | 160 ± 70 ($k_5$) | 2.4 ± 1.9 |
| P∼SKN7-R3 to YPD1 | 0.4 ± 0.1 ($k_{-8}$) | 5.0 ± 3.0 |
| P∼YPD1 to SKN7-R3 | 1.4 ± 0.2 ($k_8$) | 1.5 ± 0.5 |

[a] Rates and constants were derived from time courses for reactions between phosphorylated donor (0.25 $\mu$M) and acceptor (typically 0.125−10 $\mu$M). [b] $k_{max}$ is the maximum rate in either the forward or reverse direction (see Scheme 1). [c] There was no measurable disappearance of phospho-SSK1-R2 or appearance of phospho-YPD1 for this interaction.

of 230 ± 130 $s^{-1}$ (Figure 2, Table 1). The $K_d$ for the interaction between phospho-YPD1 and SLN1-R1 was 7.8 ± 5.7 $\mu$M.

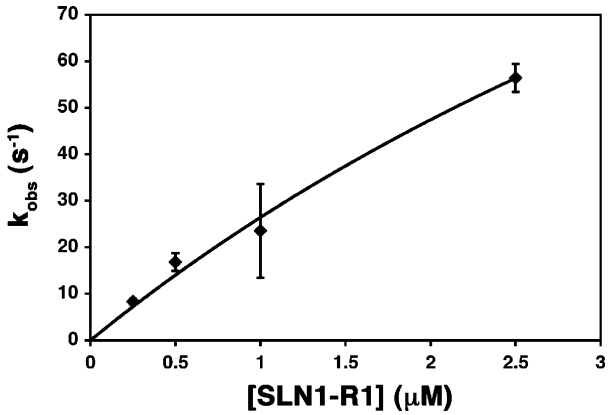


FIGURE 2: Pre-steady-state kinetics of phosphoryl transfer from phospho-YPD1 to SLN1-R1. The observed pseudo-first-order rate constant ($k_{obs}$) is plotted as a function of SLN1-R1 concentration and shows apparent saturation at high SLN1-R1 concentrations. The curve was created by fitting the data to eq 1. The error bars show the standard error of the mean.

*Phosphoryl Transfer between YPD1 and SSK1-R2 or SKN7-R3.* Phosphoryl transfer experiments using SSK1-R2, SKN7-R3, and YPD1 were carried out analogously to the experiments involving SLN1-R1 and YPD1 as described above. Isolated phospho-YPD1 (0.25 $\mu$M) was mixed with SSK1-R2 or SKN7-R3 (0.125−2.5 $\mu$M), and the values for the rate constants for these reactions were determined by following the disappearance of phospho-YPD1. The SSK1-R2 and SKN7-R3 domains can also be phosphorylated using small molecule phosphodonors, as described above for SLN1-R1, an indication that phosphoryl transfer catalytic activity primarily resides with the response regulator domain. Therefore, the single-turnover rates between phospho-YPD1 and SSK1-R2 ($k_5$) or SKN7-R3 ($k_8$) and the affinity constants were determined (Table 1). These single-turnover rate values reflect the rates when all phosphorylated YPD1 was bound by the response regulators, and there is only one phosphoryl group transfer per response regulator molecule.

When YPD1 was added to an incubation mixture containing radiolabeled phospho-SSK1-R2, no detectable amount of phosphoryl group was transferred to YPD1 (data not shown). Indeed, it has been shown previously that the phosphorylated lifetime of SSK1-R2 is dramatically stabilized (200-fold) in the presence of YPD1 and that this may be due, at least in part, to the formation of a stable complex between YPD1 and phospho-SSK1-R2, whereby YPD1 effectively shields the phosphoryl group from hydrolysis (*15*). Thus, no kinetic data were obtained for phosphotransfer between phospho-SSK1-R2 and YPD1.

In contrast to the situation with SSK1-R2, phosphoryl transfer between SKN7-R3 and YPD1 could be observed using SKN7-R3 as a phosphodonor and phosphoacceptor. The phosphoryl transfer reaction from phospho-YPD1 to SKN7-R3 exhibited a 100-fold slower single-turnover rate constant (1.4 ± 0.2 $s^{-1}$) than the phosphoryl transfer between phospho-YPD1 and SSK1-R2 (160 ± 70 $s^{-1}$) (Table 1). The transfer between phospho-SKN7-R3 and YPD1 ($k_{-8}$ = 0.4 ± 0.1 $s^{-1}$) was 70-fold slower than the phosphoryl transfer from phospho-SLN1-R1 to YPD1 ($k_2$ = 29 ± 3 $s^{-1}$). The second-order rate constant (ratio of $k_{-8}/K_d$) for the transfer involving phospho-SKN7-R3 was (8 ± 5) × $10^4$ $M^{-1}$ $s^{-1}$.

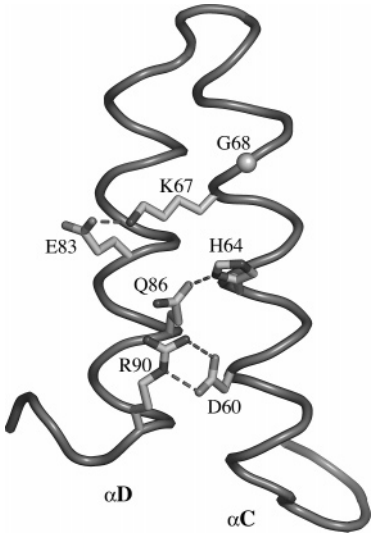


FIGURE 3: View of the αC and αD helices of YPD1. The polypeptide main chain corresponding to the αC−αD helical hairpin containing the phosphorylatable histidine residue (His 64) is shown with side chain atoms of residues relevant to this study drawn in stick model. The Cα atom of glycine 68 is shown as a sphere. Hydrogen bonds between side chain atoms are indicated by dashed lines.

*Phosphoryl Transfer between SLN1-R1 and YPD1 Mutants.* Figure 3 illustrates the three-dimensional arrangement of conserved residues surrounding the phosphorylatable histidine (His64) that were the subject of mutagenesis studies (*25*). In this previous study, the roles of these residues with respect to phosphotransfer activity and stability of the phosphohistidinyl linkage were investigated. For all the YPD1 mutants examined (K67A, R90A, G68Q, Q86A, and Q86E), steady-state levels of YPD1 phosphorylation were decreased but to varying extents depending on the mutation. However, at that time detailed kinetic studies were not carried out since the earliest time point that could be measured manually was 5 s by which time steady-state levels were already reached for all but one (G68Q) of the mutant proteins. Using the rapid-quench kinetics instrument, we investigated the kinetics of the phosphoryl transfer between SLN1-R1 and the mutant YPD1 proteins to help further define the functional roles of the conserved amino acid residues in YPD1.

All transfer reactions from phospho-SLN1-R1 to YPD1 mutants exhibited saturation kinetics at high YPD1 concentrations. The maximum forward rate constant, $k_2$, and the binding constant, $K_d$, were determined for each of the mutations and are shown in Table 2. Only the wild-type YPD1 data were fit to eq 1 where $k_{-2} \neq 0$, whereas the data obtained for the YPD1 mutants were best fit to eq 1 where $k_{-2} = 0$, indicating rapid decomposition of the product complex (with $k_3 \gg k_{-2}$). The data for phosphoryl transfer between phospho-SLN1-R1 and G68Q-YPD1 were obtained using manual mixing due to the much slower rates. Since the phosphorylated half-life of SLN1-R1 is approximately 13 min (*16*), the rate constant determined for phosphoryl transfer to the G68Q-YPD1 mutant was corrected for autodephosphorylation of phospho-SLN1-R1 that occurred during the time course of the experiment. Phosphoryl transfer between phospho-SLN1-R1 and G68Q-YPD1 was also found to be saturable; however, the saturation curve is sigmoidal

Table 2: Phosphoryl Transfer Rates and Binding Constants for Transfer between Phospho-SLN1-R1 and Wild-type and Mutant YPD1[a]

| YPD1 | $k_2$ ($s^{-1}$) | $K_d$ ($\mu$M) | $k$[b] ($M^{-1}s^{-1}$) |
|---|---|---|---|
| wild-type | $29 \pm 3$ | $1.4 \pm 0.3$ | $21 \times 10^6$ |
| K67A | $33 \pm 4$ | $4.2 \pm 1.5$ | $7.9 \times 10^6$ |
| R90A | $11 \pm 1$ | $1.4 \pm 0.6$ | $7.9 \times 10^6$ |
| Q86A | $1.7 \pm 0.3$ | $1.4 \pm 0.8$ | $1.2 \times 10^6$ |
| Q86E | $36 \pm 4$ | $2.1 \pm 0.5$ | $17 \times 10^6$ |
| G68Q | 0.003[c] | ~2[d] | $\sim 1.5 \times 10^4$ |

[a] Rates and constants were derived from time courses for reactions between phospho-SLN1−R1 (0.25 $\mu$M) and YPD1 (0.125−4 $\mu$M). [b] $k$ is the limiting second-order rate constant and was calculated using the ratio of $k_2/K_d$. [c] The rate constant for the G68Q transfer was determined using manual mixing. [d] The dissociation constant was estimated from the hyperbolic portion of Figure 4.

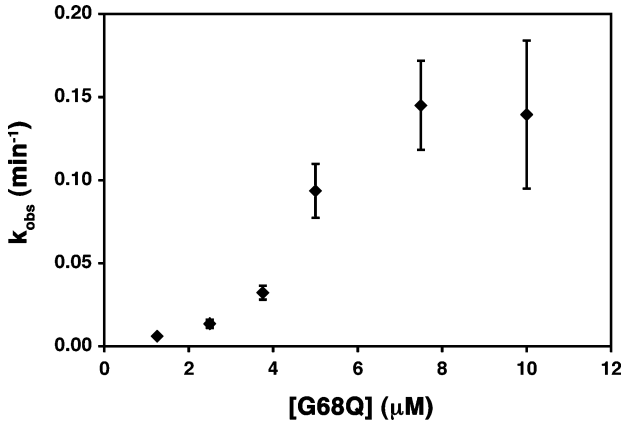


FIGURE 4: Pre-steady-state kinetics of phosphoryl transfer from phospho-SLN1-R1 to G68Q-YPD1. The observed pseudo-first-order rate constant ($k_{obs}$) is plotted as a function of G68Q-YPD1 concentration and shows saturation at high G68Q-YPD1 concentrations. The error bars show the standard error of the mean.

(Figure 4). The phospho-SLN1-R1 preparation contains a significant portion of unphosphorylated SLN1-R1 (~90%). Thus, at low concentrations, the G68Q-YPD1 mutant may bind tighter to unphosphorylated SLN1-R1, effectively competing with binding and phosphotransfer involving phospho-SLN1-R1. Only at high G68Q-YPD1 concentrations would there be sufficient free G68Q-YPD1 to interact with phospho-SLN1-R1. The phosphotransfer rate itself is very slow compared to wild-type YPD1, with a maximal forward rate constant of 0.003 $s^{-1}$ (Table 2). Due to the sigmoidal nature of the data, the forward rate constant was determined manually and the dissociation constant, estimated on the basis of the hyperbolic portion of Figure 4, is 2 $\mu$M.

*Effect of YPD1 Mutations on Phosphoryl Transfer between Phospho-YPD1 and SSK1-R2.* Based on the effect of the mutated residues K67A, R90A, and Q86A of YPD1 on the forward rate, affinity between phospho-SLN1-R1 and YPD1, or both, we also determined kinetic constants for the phosphoryl transfer between these YPD1 mutants and SSK1-R2 using the rapid-quench kinetics instrument. For these mutants, the rate constants ($k_5$) for the single-turnover experiment from phospho-YPD1 to SSK1-R2 were within experimental error of each other and of those of wild-type YPD1 (Table 3). The phosphoryl transfer between phospho-G68Q-YPD1 and SSK1-R2 was monitored using manual mixing, since the half-life of the reaction was slower than 10 s. The maximal forward rate constant determined for this

Table 3: Phosphoryl Transfer Rates for Transfer between Phospho-YPD1 and SSK1-R2[a]

| P∼YPD1 | $k_5$ ($s^{-1}$) |
|---|---|
| wild-type | 160 ± 70 |
| K67A | 130 ± 30 |
| R90A | 170 ± 40 |
| Q86A | 120 ± 20 |
| G68Q | 0.24 ± 0.06 |

[a] Rates were derived from time courses for reactions between phospho-YPD1 (0.25 $\mu$M) and SSK1-R2 (0.25−5 $\mu$M).

reaction was 0.24 $s^{-1}$. No evidence of inhibition was observed for the phosphotransfer reaction between phospho-YPD1 and SSK1-R2.

## DISCUSSION

Despite the hundreds of two-component regulatory systems that have been identified in prokaryotes and eukaryotes, only a small number of bacterial phosphotransfer systems have been investigated in detail using kinetic studies (*20*, *26*−*28*). These studies involved phosphoryl transfer from histidine kinases to response regulator domains. Here we have investigated the phosphotransfer kinetics of the eukaryotic yeast osmoregulation phosphorelay in vitro using a rapid-quench kinetics instrument. The isolated response regulator domains from SLN1, SSK1, and SKN7 have been used to examine phosphoryl transfer between the individual response regulator domains and the HPt protein YPD1. In addition, the effect of YPD1 mutations on phosphotransfer to and from the response regulators (RR) was examined. Data were analyzed using Scheme 1.

*Significance of YPD1-Dependent Phosphotransfer Kinetics in Osmoregulation in Yeast.* The kinetic data obtained in this study showed that the rates of phosphoryl transfer were saturable at high protein concentration, which suggests the formation of a complex, YPD1∼P·RR. The transfer between SLN1-R1 and YPD1 and the transfer between SKN7-R3 and YPD1 are reversible. In contrast, phosphotransfer from YPD1 to SSK1-R2 is strongly favored, and no reverse reaction, that is, transfer from SSK1-R2∼P to YPD1, was observed, suggesting either very low affinity for the YPD1·SSK1-R2∼P complex or a very low value for $k_{-5}$. A previous qualitative binding study supports the latter interpretation (*15*). Measurement of the observed rate constants for the individual reactions as a function of "substrate" (phosphoacceptor) concentration provided the maximum forward rate constants, $k_{max}$, at saturating "substrate" concentration, as well as a measure of the binding affinity, $K_d$, between the phosphodonor and phosphoacceptor proteins. These quantitative data provided a basis for comparison of the phosphotransfer reactions between YPD1 and the three response regulator domains within the yeast phosphorelay. Phosphotransfer between SLN1-R1 and YPD1 and the transfer between YPD1 and SSK1-R2 were observed to be very rapid ($k_2$ and $k_5$, respectively, Table 1). In contrast, the transfer between YPD1 and SKN7-R3 is at least an order of magnitude slower (compare $k_8$ with $k_5$ and $k_2$, Table 1). The binding affinities for the complexes between YPD1 and phospho-SLN1-R1 and phospho-SKN7-R3 were about the same within the standard errors. The value for the second-order rate constant for the phosphoryl transfer between SLN1-R1 and YPD1 ($k = 2 \times 10^7$ $M^{-1}$ $s^{-1}$) suggests a near diffusion-limited reaction. In contrast, the second-order rate constant for the phosphoryl transfer between SKN7-R3 and YPD1 is 260-fold lower.

A finite value of $k_{-2}$ is observed only for phosphoryl transfer from SLN1-R1∼P to YPD1. An apparent value of 7.5 $s^{-1}$ is estimated for $k_{-2,obs}$ in this case (Figure 1B). This rate constant is not, however, necessarily the intrinsic rate constant for transfer of phosphate in the reverse direction (from YPD1∼P to SLN1-R1), since it depends on the partitioning of the SLN1-R1·YPD1∼P complex in the direction of phosphoryl transfer ($k_{-2}$) as opposed to dissociation ($k_3$, Scheme 1). The true value of $k_{-2}$ must be at least 230 $s^{-1}$ (Table 1) or greater, the single-turnover value measured in the reverse reaction experiment (Table 1). Once the SLN1-R1·YPD1∼P product complex is formed from the SLN1-R1∼P·YPD1 reactant complex, it can partition toward reactants with rate constant $k_{-2}$ or dissociate with rate constant $k_3$. The rate of formation of the reactant complex will depend on the concentration of SLN1-R1·YPD1∼P, which depends on the rate constant for dissociation, $k_3$, compared to that for the reverse phosphoryl transfer, $k_{-2}$. The observed value of $k_{-2,obs}$ measured from Figure 1B is 7.5 $s^{-1}$, and this can be compared to the value of 230 $s^{-1}$ measured for $k_{-2}$ in the reverse reaction experiment. Thus, in the forward phosphotransfer reaction between SLN1-R1∼P and YPD1, the rate of product complex dissociation, $k_3$, is much faster than the rate of reverse phosphoryl transfer, $k_{-2}$, and therefore reduces the rate of $k_{-2}$ to $k_{-2,obs}$. The partition ratio for SLN1-R1·YPD1∼P is equal to $k_{-2}/(k_3 + k_{-2})$, and since $k_3 \gg k_{-2}$, this reduces to $k_{-2}/k_3$. This will be approximately equal to the fraction of the product complex that gives the reactant complex and is thus also equal to the ratio of $k_{-2,obs}$ and $k_{-2}$ (7.5 $s^{-1}$/230 $s^{-1}$), or 0.03; that is, once formed, 97% of the complex dissociates to give YPD1∼P. On the basis of the analysis above, the rate of dissociation ($k_3$) of SLN1-R1·YPD1∼P is about 30 times faster than the rate of reverse phosphoryl transfer ($k_{-2}$), consistent with the role of YPD1 as a phosphorelay protein. The value of $k_3$ is then at least 6900 $s^{-1}$. Given a $K_d$ of about 8 $\mu$M in the direction of SLN1-R1 phosphorylation, a value of about 9 $\times 10^8$ $M^{-1}$ $s^{-1}$ is estimated for $k_{-3}$, a reasonable value for the rate of diffusion of YPD1∼P and SLN1-R1 together to give the SLN1-R1·YPD1∼P complex (*34*). In the case of phosphotransfer between YPD1 and SKN7-R3, the value for $k_{-7}$ is much greater than $k_8$. On the basis of the similarity in $K_d$ values for SKN7-R3 and SLN1-R1, the difference between the two enzymes appears to reside in the rate of the catalytic step. The values of $k_{-8}$ and $k_8$ are decreased by 70-fold and 160-fold, respectively, for SKN7-R3 relative to the corresponding values for SLN1-R1 ($k_2$ and $k_{-2}$). The 70-fold difference between $k_{-8}$ and $k_2$ represents a transition state for phosphoryl transfer that is 2.5 kcal/mol higher in energy for SKN7-R3 than for SLN1-R1. The difference in $K_{eq}$ for the chemical steps, 0.7 for SLN1-R1 and 0.08 for SKN7-R3, also reflects the differences in the flux of phosphoryl groups through the phosphorelay system. Given the estimated equilibrium constants, one can calculate the equilibrium concentrations of reactants and products beginning with any phosphodonor and phosphoacceptor concentration. For example, in the phosphotransfer experiment starting with equimolar concentrations of phospho-SLN1-

R1 and YPD1, the calculated values for the equilibrium concentrations of phospho-SLN1-R1 and phospho-YPD1 are 55% and 45%, respectively, using the $K_{eq}$ of 0.7 for the SLN1-R1 catalyzed reaction. These values can be compared with the experimental equilibrium concentrations of phospho-SLN1-R1 and phospho-YPD1, which are about 50% each (*25*). Within error (approximately 50% on the equilibrium constant), the calculated and experimental concentrations agree well.

Overall, under our experimental conditions, phosphorelay favors rapid formation of phospho-SSK1-R2 over formation of phospho-SKN7-R3. This is consistent with the function of the SLN1−YPD1−SSK1 phosphorelay under normal osmotic conditions in vivo, when SSK1 has to be maintained in its inactive phosphorylated form to prevent activation of the downstream MAPK cascade (*6*). Furthermore, under the conditions tested, we have not observed reverse phosphotransfer from SSK1-R2 to YPD1, which is consistent with other qualitative evidence that shows that YPD1 and phospho-SSK1-R2 form a stable complex that prevents hydrolysis of the aspartyl phosphate linkage on SSK1-R2 (*15*). Taken together, these data help to explain how SSK1-R2 is maintained in its phosphorylated form under normal cellular growth conditions. However, the mechanism by which SSK1 becomes rapidly dephosphorylated when cells experience hyperosmotic stress is currently not understood. Some, but not all, of the SKN7-associated cellular responses are dependent on phosphorylation of its response regulator domain, that is, cell cycle regulation, cell wall synthesis, and osmotic stress response (*11*, *13*, *35*). Furthermore, SKN7 has been localized to the nucleus, whereas YPD1 is distributed throughout the cytosol and nucleus (*8*, *9*, *36*). The rapid phosphorelay from SLN1-R1 to SSK1-R2 via the YPD1 branchpoint under normal osmolarity conditions is supported by the present data. However, the regulation of phosphoryl transfer from YPD1 to SKN7 is apparently more complex than the seemingly straightforward cytosolic phosphotransfer between YPD1 and SSK1.

*Function of Individual Conserved YPD1 Residues.* In a previous study, four amino acid residues in YPD1 (K67, G68, Q86, R90) that are highly conserved among HPt domains were mutated to alanine (K67, Q86, R90), glutamine (G68), or glutamic acid (Q86) to examine the role of these residues in phosphoryl transfer reactions (*25*). The results of phosphoryl transfer reactions between SLN1-R1 and these YPD1 mutants revealed that each mutant to a varying degree showed a decrease in steady-state levels of phosphorylation ranging from about 20−45% of wild-type levels. Together with the known X-ray structure of YPD1, these results suggest that K67 on the αC-helix (within ionic bonding distance to E83 on the αD-helix) is involved in proper positioning of the αC- and αD-helices relative to each other, while R90 on the αD-helix (within ionic bonding distance to D60 on the αC-helix) is involved in positioning the helices but may also participate in electrostatic stabilization of the phosphorylated histidine (Figure 3). The glutamine residue at position 86 is involved in hydrogen bonding with the imidazole ring of H64, presumably to properly orient the imidazole for phosphoryl transfer.

The K67A and R90A mutant proteins differ in their behavior relative to each other. The K67A mutant protein exhibits approximately a 3-fold increase in $K_d$ and thus affects the binding of YPD1 to SLN1-R1∼P, while the R90A mutant protein shows about a 2.5-fold decrease in $k_2$ suggesting an effect on the phosphoryl transfer rate. No difference, however, is observed in the phosphorylation of SSK1-R2. The decrease in binding affinity upon elimination of the K67 side chain is fully consistent with the location and proposed function of the residue. The modest (0.65 kcal/mol) decrease in binding energy can be explained by a slight shift in the position of the αC and αD helices. Once bound, however, phosphoryl transfer occurs with an efficiency equal to the wild-type protein. Mutation of R90 to alanine gives results that are consistent with its participation in stabilizing phospho-H64. A role similar to that played by K67 cannot, however, be ruled out, with binding identical to wild-type, but a change in orientation of the histidine nucleophile giving a 3-fold decrease in $k_2$. Discerning which of these possibilities is correct will have to await further study.

The 17-fold decrease in $k_2$ observed with the Q86A mutant suggests either a role in orientation of H64, a modulation of the imidazole nucleophilicity, or both. Interestingly, several HPt proteins have a glutamic acid residue rather than a glutamine residue located in this position. For YPD1, the slight increase in $k_2$ ($1.24 \pm 0.17\ s^{-1}$) upon substitution of Q86 with glutamic acid suggests that the glutamine side chain both enhances the nucleophilicity of the imidazole and is likely involved in orientation as well. Again, once phosphorylated, no change in its behavior as a phosphodonor to SSK1-R2 is noted.

No change in the rate of phosphorylation of SSK1-R2 using any of the mutant YPD1 proteins was observed, with the exception of the drastic change for the G68Q mutant. Data are consistent with a difference, albeit perhaps subtle, in the orientation between phosphoryl donor and acceptor in the SLN1-R1 and SSK1-R2 complexes with YPD1.

The recently available cocrystal structure of the YPD1/SLN1-R1 complex (*37*) may help explain some of the findings presented here. The YPD1 residues Q86, R90, and D60 (which is associated with R90 via a hydrogen bond) are all shown to interact through a hydrogen bond network with a conserved glutamine residue (Q1146) located in the β3-α3 loop of SLN1-R1. This loop contributes to formation of the active site in the response regulator domain. All together, these residues may provide a hydrogen bond network facilitating proper alignment between SLN1-R1 and YPD1 for phosphoryl transfer. Thus any mutation that disrupts a hydrogen bond within this network may cause a misalignment in the active site and result in a slower transfer rate. Moreover, in the YPD1 structure, K67 forms an interhelical ionic bond with E83, and in the structure of the YPD1/SLN1-R1 complex, the side chain Cγ atom from residue E83 in YPD1 also makes contact to a phenylalanine side chain (F1175) of SLN1-R1 located in the β4-α4 loop. In contrast to the interactions mentioned above, this interaction is hydrophobic in nature and contributes to the binding interface between SLN1-R1 and YPD1. Thus, the K67A-YPD1 mutant is affected in its binding to SLN1-R1 as indicated by the increased $K_d$ value (Table 2). Of the mutant YPD1 proteins studied (Tables 2 and 3), only three give significant changes in the value of $k_2$, R90A (∼3-fold decrease), Q86A (∼17-fold decrease), and G68Q (∼9700-fold decrease), but only K67A exhibited a significant increase in $K_d$ (∼3-fold).

The G68Q mutation is perhaps easiest to understand, since the glycine is located on the same face of the αC helix as H64 and replacement of the small side chain with a propionamide results in significant steric hindrance, which we postulated may affect protein−protein interactions, phosphorylation of H64, or both (*25*). The dramatic reduction in phosphotransfer rates either from SLN1-R1 to the G68Q-YPD1 mutant (9700-fold) or from G68Q-YPD1 to SSK1-R2 (680-fold) is most likely due to improper alignment of the phosphoryl group with regard to the positioning of the two proteins.

*Comparison to Other Phosphoryl Transfer Systems.* To date, there are three two-component systems that have been studied in detail at the kinetic level: (i) the VanS to VanR transfer of the vancomycin resistance system in *Enterococcus faecium* (*28*), (ii) the CheA to CheY transfer of the *Escherichia coli* chemotaxis system (*20*, *21*, *27*, *38*), and (iii) the KinA−Spo0F−Spo0B−Spo0A phosphorelay, which is involved in sporulation in *Bacillus subtilis* (*26*). We have presented here the first kinetic study of a eukaryotic two-component phosphorelay system, which will allow us to compare the kinetic features between the bacterial and eukaryotic systems.

The phosphotransfer from the histidine kinase VanS to the response regulator VanR in the vancomycin resistance system is similar to the yeast phosphorelay reactions in that the rate is saturable at high VanR concentrations. The forward rate constant for the phosphoryl transfer was measured to be 1.6 $s^{-1}$. However, the VanS/VanR transfer reaction is not reversible and thus behaves more like the yeast phosphorelay system with respect to transfer to SSK1-R2. Interestingly, VanR was found to have a higher affinity for unphosphorylated VanS, forming a nonproductive complex and thus inhibiting the phosphoryl transfer at low substrate concentrations, similar to behavior of the G68Q mutant of YPD1 as an acceptor of phosphoryl groups from SLN1-R1∼P.

In the bacterial chemotaxis system, phosphotransfer from the histidine kinase CheA to the response regulator CheY was reversible as well as saturable. The maximal transfer rate for the CheA/CheY transfer was 750 $s^{-1}$ (25 times faster than transfer from SLN1-R1 to YPD1) with a second-order rate constant of ∼$10^8$ $M^{-1}$ $s^{-1}$, an order of magnitude faster than that of the yeast phosphorelay system (*20*, *27*). The histidine kinase CheA contains two domains at its N-terminus that are important for the phosphoryl transfer to CheY: the P1 domain, which is functionally and structurally equivalent to YPD1 and thereby functions as an HPt domain, and the P2 domain, which contains a CheY binding site and presumably helps to position CheY in proximity to the phosphorylated histidine in the P1 domain (*24*, *39*−*41*). Phosphoryl transfer from a mutant CheA that lacks the P2-CheY binding domain (CheAΔP2), as well as a CheA mutant that only consists of the P1 domain to CheY, has been shown to occur with second-order rate constants of $1.5 \times 10^6$ and $2.3 \times 10^6$ $M^{-1}$ $s^{-1}$, respectively (*38*). These rate constants are 100-fold lower than the one determined for the wild-type CheA/CheY phosphoryl transfer, indicating that both the P1 and P2 domain of CheA contribute to the rapid phosphoryl transfer to CheY. For comparison, phosphorylation of CheY by small molecule phosphodonors was even slower with second-order rate constants of 5−50 $M^{-1}$ $s^{-1}$ (*20*, *21*, *33*). Most recently the kinetics of the association of the CheA-P2 domain and CheY have been examined further in the absence of phosphotransfer using fluorescence spectroscopy (*42*). These studies revealed a very rapid association reaction with $k_{assn} \approx 10^8$ $M^{-1}$ $s^{-1}$ and further support the idea that the P2 domain evolved to facilitate rapid association of CheA and CheY. However, the speed of the chemical phosphotransfer step may reside in the CheA-P1 (HPt-like) domain, CheY, or both (*42*). At present it is not known whether the N-terminal histidine kinase domain in SLN1 influences in any way the kinetics of phosphoryl transfer from SLN1-R1 to YPD1.

Data obtained for both the VanS/VanR and CheA/CheY systems support the formation of a complex between phosphodonor and phosphoacceptor protein prior to the chemical transfer of the phosphoryl group. The differences in the phosphotransfer rates appear to reflect the response time of the organism to environmental signals. The maximal transfer rate for the CheA/CheY transfer ($k_2$ = 750 $s^{-1}$) permits signal transduction within milliseconds to rapidly modify the movement of swimming cells. In contrast, the VanS/VanR system serves to regulate gene expression over a much longer time, which is reflected in its significantly slower phosphoryl transfer rate ($k_2$ = 1.6 $s^{-1}$).

The *B. subtilis* phosphorelay system that activates sporulation involves the two response regulators Spo0F and Spo0A and the HPt protein Spo0B. Due to the experimental setup, kinetic data for the complete phosphorelay from preformed phospho-Spo0F to Spo0A via Spo0B were determined. The transfer rate for the complete phosphorelay system was 0.2 $s^{-1}$. This relatively slow transfer rate reflects the function of this signal transduction system, which serves to regulate gene expression leading to sporulation, a process that occurs over a relatively long time period.

The yeast SLN1−YPD1−SSK1 phosphorelay serves to maintain the HOG1 MAPK cascade in an inactive state under normal osmotic conditions. The rate of the phosphoryl transfer between the response regulator domains of both SLN1 and SSK1 and the HPt protein YPD1 was relatively fast (29 and 160 $s^{-1}$, respectively**)** in comparison to the bacterial VanS/VanR and sporulation systems, which is indicative of the need to keep SSK1 phosphorylated. We have previously determined that YPD1 stabilizes the half-life of phosphorylated SSK1-R2 nearly 200-fold (*15*). Together with the rapid phosphotransfer from SLN1-R1 to YPD1 to SSK1-R2, this ensures that the response regulator is maintained in the phosphorylated form in vitro. Thus, a high transfer rate like the one seen in the CheA/CheY transfer is not needed in the yeast system since YPD1·SSK1∼P complex formation may be an additional mechanism that ensures SSK1 remains phosphorylated under nonosmotic stress conditions. When yeast cells are exposed to hyperosmotic shock, SSK1 must be dephosphorylated for the downstream HOG1 MAPK cascade to be activated (*3*, *4*, *6*). HOG1 phosphorylation has been observed to occur within minutes of osmotic upshift, whereas the recovery time post-osmotic shock is about 15−20 min during which HOG1 is dephosphorylated, SSK1 is degraded, and newly synthesized SSK1 presumably is phosphorylated via the SLN1−YPD1 phosphorelay (*43*−*45*). This raises the question: how is the SLN1−YPD1−SSK1 phosphorelay system temporally and environmentally regulated? One possibility is that the rate

of phosphoryl transfer to SSK1 is decreased in response to osmotic stress and the YPD1·SSK1∼P complex subsequently dissociates or changes conformation thus permitting hydrolysis of the aspartyl phosphate linkage. The presence of a yet to be identified aspartyl phosphatase that dephosphorylates SSK1 in response to hyperosmotic stress also cannot be ruled out. Additional kinetic studies as well as direct examination of the in vivo phosphorylation state of SSK1 in complex with YPD1 will be required to address this question.

## ACKNOWLEDGMENT

We thank members of the West laboratory and Dali Liu for critical reading of the manuscript, Jennifer Gray for expert technical assistance, and Stace Porter for help in figure preparation.

## REFERENCES

1. West, A. H., and Stock, A. M. (2001) Histidine kinases and response regulator proteins in two-component signaling systems, *Trends Biochem. Sci. 26*, 369−376.
2. Appleby, J. L., Parkinson, J. S., and Bourret, R. B. (1996) Signal transduction via the multistep phosphorelay: not necessarily a road less traveled, *Cell 86*, 845−848.
3. Maeda, T., Wurgler-Murphy, S. M., and Saito, H. (1994) A two-component system that regulates an osmosensing MAP kinase cascade in yeast, *Nature 369*, 242−245.
4. Posas, F., Wurgler-Murphy, S. M., Maeda, T., Witten, E. A., Thai, T. C., and Saito, H. (1996) Yeast HOG1 MAP kinase cascade is regulated by a multistep phosphorelay mechanism in the SLN1−YPD1-SSK1 "two-component" osmosensor, *Cell 86*, 865−875.
5. Saito, H. (2001) Histidine phosphorylation and two-component signaling in eukaryotic cells, *Chem. Rev. 101*, 2497−2509.
6. Posas, F., and Saito, H. (1998) Activation of the yeast SSK2 MAP kinase kinase kinase by the SSK1 two-component response regulator, *EMBO J. 17*, 1385−1394.
7. Mager, W. H., and Varela, J. C. S. (1993) Osmostress response of the yeast *Saccharomyces*, *Mol. Microbiol. 10*, 253−258.
8. Brown, J. L., Bussey, H., and Stewart, R. C. (1994) Yeast Skn7p functions in a eukaryotic two-component regulatory pathway, *EMBO J. 13*, 5186−5194.
9. Raitt, D. C., Johnson, A. L., Erkine, A. M., Makino, K., Morgan, B., Gross, D. S., and Johnston, L. H. (2000) The Skn7 response regulator of *Saccharomyces cerevisiae* interacts with Hsf1 in vivo and is required for the induction of heat shock genes by oxidative stress, *Mol. Biol. Cell 11*, 2335−2347.
10. Morgan, B. A., Banks, G. R., Toone, W. M., Raitt, D., Kuge, S., and Johnston, L. H. (1997) The Skn7 response regulator controls gene expression in the oxidative stress response of the budding yeast *Saccharomyces cerevisiae*, *EMBO J. 16*, 1035−1044.
11. Li, S., Dean, S., Li, Z., Horecka, J., Deschenes, R. J., and Fassler, J. S. (2002) The eukaryotic two-component histidine kinase Sln1p regulates OCH1 via the transcription factor, Skn7p, *Mol. Biol. Cell 13*, 412−424.
12. Li, S., Ault, A., Malone, C. L., Raitt, D., Dean, S., Johnston, L. H., Deschenes, R. J., and Fassler, J. S. (1998) The yeast histidine protein kinase, Sln1p, mediates phosphotransfer to two response regulators, Ssk1p and Skn7p, *EMBO J. 17*, 6952−6962.
13. Brown, J. L., North, S., and Bussey, H. (1993) *SKN7*, a yeast multicopy suppressor of a mutation affecting cell wall $\beta$-glucan assembly, encodes a product with domains homologous to prokaryotic two-component regulators and to heat shock transcription factors, *J. Bacteriol. 175*, 6908−6915.
14. Morgan, B. A., Bouquin, N., Merrill, G. F., and Johnston, L. H. (1995) A yeast transcription factor bypassing the requirement for SBF and DSC1/MBF in budding yeast has homology to bacterial signal transduction proteins, *EMBO J. 14*, 5679−5689.
15. Janiak-Spens, F., Sparling, D. P., and West, A. H. (2000) Novel role for an HPt domain in stabilizing the phosphorylated state of a response regulator domain, *J. Bacteriol. 182*, 6673−6678.
16. Janiak-Spens, F., Sparling, J. M., Gurfinkel, M., and West, A. H. (1999) Differential stabilities of phosphorylated response regulator domains reflect functional roles of the yeast osmoregulatory SLN1 and SSK1 proteins, *J. Bacteriol. 181*, 411−417.
17. Stock, A. M., Robinson, V. L., and Goudreau, P. N. (2000) Two-component signal transduction, *Annu. Rev. Biochem. 69*, 183−215.
18. Stock, A. M., and West, A. H. (2002) in *Histidine kinases in signal transduction* (Inouye, M., and Dutta, R., Eds.) pp 237−271, Academic Press, New York.
19. Lukat, G. S., McCleary, W. R., Stock, A. M., and Stock, J. B. (1992) Phosphorylation of bacterial response regulator proteins by low molecular weight phospho-donors, *Proc. Natl. Acad. Sci. U.S.A. 89*, 718−722.
20. Mayover, T. L., Halkides, C. J., and Stewart, R. C. (1999) Kinetic characterization of CheY phosphorylation reactions: Comparison of P−CheA and small-molecule phosphodonors, *Biochemistry 38*, 2259−2271.
21. Silversmith, R. E., Appleby, J. L., and Bourret, R. B. (1997) Catalytic mechanism of phosphorylation and dephosphorylation of CheY: Kinetic characterization of imidazole phosphates as phosphodonors and the role of acid catalysis, *Biochemistry 36*, 14965−14974.
22. Xu, Q., and West, A. H. (1999) Conservation of structure and function among histidine-containing phosphotransfer (HPt) domains as revealed by the crystal structure of YPD1, *J. Mol. Biol. 292*, 1039−1050.
23. Song, H. K., Lee, J. Y., Lee, M. G., Min, J. M. K., Yang, J. K., and Suh, S. W. (1999) Insights into eukaryotic multistep phosphorelay signal transduction revealed by the crystal structure of Ypd1p from *Saccharomyces cerevisiae*, *J. Mol. Biol. 293*, 753−761.
24. Mourey, L., Da Re, S., Pédelacq, J.-D., Tolstykh, T., Faurie, C., Guillet, V., Stock, J. B., and Samama, J.-P. (2001) Crystal structure of the CheA histidine phosphotransfer domain that mediates response regulator phosphorylation in bacterial chemotaxis, *J. Biol. Chem. 276*, 31074−31082.
25. Janiak-Spens, F., and West, A. H. (2000) Functional roles of conserved amino acid residues surrounding the phosphorylatable histidine of the yeast phosphorelay protein YPD1, *Mol. Microbiol. 37*, 136−144.
26. Grimshaw, C. E., Huang, S., Hanstein, C. G., Strauch, M. A., Burbulys, D., Wang, L., Hoch, J. A., and Whiteley, J. M. (1998) Synergistic kinetic interactions between components of the phosphorelay controlling sporulation in *Bacillus subtilis*, *Biochemistry 37*, 1365−1375.
27. Stewart, R. C. (1997) Kinetic characterization of phosphotransfer between CheA and CheY in the bacterial chemotaxis signal transduction pathway, *Biochemistry 36*, 2030−2040.
28. Fisher, S. L., Kim, S.-K., Wanner, B. L., and Walsh, C. T. (1996) Kinetic comparisons of the specificity of the vancomycin resistance kinase VanS for two response regulators, VanR and PhoB, *Biochemistry 35*, 4732−4740.
29. Xu, Q., Nguyen, V., and West, A. H. (1999) Purification, crystallization, and preliminary X-ray diffraction analysis of the yeast phosphorelay protein YPD1, *Acta Crystallogr. D55*, 291−293.
30. Guan, K. L., and Dixon, J. E. (1991) Eukaryotic proteins expressed in *Escherichia coli*: An improved thrombin cleavage and purification procedure of fusion proteins with glutathione *S*-transferase, *Anal. Biochem. 192*, 262−267.
31. Zapf, J. W., Hoch, J. A., and Whiteley, J. M. (1996) A phosphotransferase activity of the *Bacillus subtilis* sporulation protein Spo0F that employs phosphoramidate substrates, *Biochemistry 35*, 2926−2933.
32. Lukat, G. S., Stock, A. M., and Stock, J. B. (1990) Divalent metal ion binding to the CheY protein and its significance to phosphotransfer in bacterial chemotaxis, *Biochemistry 29*, 5436−5442.
33. Da Re, S. S., Deville-Bonne, D., Tolstykh, T., Véron, M., and Stock, J. B. (1999) Kinetics of CheY phosphorylation by small molecule phosphodonors, *FEBS Lett. 457*, 323−326.
34. Fersht, A. (1999) *Structure and mechanism in protein science*, W. H. Freeman and Company, New York.
35. Ketela, T., Brown, J. L., Stewart, R. C., and Bussey, H. (1998) Yeast Skn7p activity is modulated by the Sln1p-Ypd1p osmosensor and contributes to regulation of the HOG1 pathway, *Mol. Gen. Genet. 259*, 372−378.

36. Lu, J. M.-Y., Deschenes, R. J., and Fassler, J. S. (2003) *Saccharomyces cerevisiae* histidine phosphotransferase Ypd1p shuttles between the nucleus and cytoplasm for *SLN1*-dependent phosphorylation of Ssk1p and Skn7p, *Eukaryotic Cell 2*, 1304−1314.
37. Xu, Q., Porter, S. W., and West, A. H. (2003) The yeast YPD1/SLN1 complex: Insights into molecular recognition in two-component systems, *Structure 11*, 1569−1581.
38. Stewart, R. C., Jahreis, K., and Parkinson, J. S. (2000) Rapid phosphotransfer to CheY from a CheA protein lacking the CheY-binding domain, *Biochemistry 39*, 13157−13165.
39. Swanson, R. V., Schuster, S. C., and Simon, M. I. (1993) Expression of CheA fragments which define domains encoding kinase, phosphotransfer, and CheY binding activities, *Biochemistry 32*, 7623−7629.
40. Li, J., Swanson, R. V., Simon, M. I., and Weis, R. M. (1995) The response regulators CheB and CheY exhibit competitive binding to the kinase CheA, *Biochemistry 34*, 14626−14636.
41. Hess, J. F., Oosawa, K., Kaplan, N., and Simon, M. I. (1988) Phosphorylation of three proteins in the signaling pathway of bacterial chemotaxis, *Cell 53*, 79−87.
42. Stewart, R. C., and Van Bruggen, R. (2004) Association and dissociation kinetics for CheY interacting with the P2 domain of CheA, *J. Mol. Biol. 336*, 287−301.
43. Brewster, J. L., de Valoir, T., Dwyer, N. D., Winter, E., and Gustin, M. C. (1993) An osmosensing signal transduction pathway in yeast, *Science 259*, 1760−1763.
44. Maeda, T., Takekawa, M., and Saito, H. (1995) Activation of yeast PBS2 MAPKK by MAPKKKs or by binding of an SH3-containing osmosensor, *Science 269*, 554−558.
45. Sato, N., Kawahara, H., Toh-e, A., and Maeda, T. (2003) Phosphorelay-regulated degradation of the yeast Ssk1p response regulator by the ubiquitin-proteosome system, *Mol. Cell. Biol. 23*, 6662−6671.

BI048433S